

## Water Vapor–Induced OLR Variations Associated with High Cloud Changes over the Tropics: A Study from *Meteosat-5* Observations

BYUNG-JU SOHN

*School of Earth and Environmental Sciences, Seoul National University, Seoul, Korea*

JOHANNES SCHMETZ

*European Organization for the Exploitation of Meteorological Satellites, Darmstadt, Germany*

(Manuscript received 13 May 2003, in final form 21 November 2003)

### ABSTRACT

Subdividing the Indian Ocean domain into three areas: (i) a moist cloudy area due to tropical deep convection, (ii) a moist clear area fed by the evaporation of hydrometeors from adjacent high clouds, and (iii) a dry area represented by descending air over the subtropics, the relationships between upper-tropospheric humidity over these three areas and tropical convections are examined using the *European Geostationary Meteorological Satellite (Meteosat-5)* observations. It is observed that the clear dry area shrinks and becomes drier in response to expansion of the cloudy area in the Tropics and vice versa. This change in upper-tropospheric humidity over the subtropics appears to mitigate the increase (decrease) in water vapor greenhouse effect caused by the expansion (contraction) of moist convective areas.

A simple sensitivity test shows that the strength of the water vapor feedback due to changes in the spatial extent of tropical convection is benign, though slightly negative, if the changes in subtropical dryness are considered.

### 1. Introduction

It is well known that water vapor is the most important greenhouse gas in the atmosphere. In recent years much effort has been made to better understand the water vapor feedback in the earth's climate system. Present climate model estimates suggest that water vapor feedback brings about an increased climate sensitivity by a factor of 2 (Houghton et al. 2001). This is largely explained by the notion that the atmosphere can hold more water vapor at higher temperatures, which in turn increases the trapping of infrared radiation, as shown in the strong observed correlation between total precipitable water and SST over the ocean (Raval and Ramanathan 1989; Stephens 1990; Inamadar and Ramanathan 1998).

While the total water vapor amount in the atmosphere is the first-order element describing the water vapor greenhouse effect, it is important to note that changes in the vertical distribution of water vapor is also a factor influencing the overall water vapor greenhouse effect. This is due to the vertical redistribution of water vapor caused by tropical convection. In particular the upper

troposphere can give a high and variable impact on radiation balance since the effectiveness of water vapor as a tropospheric greenhouse gas increases rapidly with altitude due to the decrease of temperature with height (Schmetz et al. 1995). This in turn can also influence the environment in favor of deep convection (e.g., Larson et al. 1999). The implication of the longwave radiation balance on the large-scale circulation has been emphasized in many studies also highlighting the importance of the large-scale linkage between cloud cover and water vapor (Soden and Fu 1995; Udelhofen and Hartmann 1995; Sherwood 1999; Larson et al. 1999; Sassi et al. 2001), leading to a notion that upper-tropospheric moisture is fed by convection. To this end supporting evidence has been provided by Schmetz et al. (1995) who further showed a distinct relationship between monthly mean upper-tropospheric humidity and large-scale divergence.

More recently, by separating the tropical area into moist cloudy, moist clear, and dry areas, Lindzen et al. (2001, hereafter LCH) studied impact of water vapor redistribution owing to relative changes in the fractional areas of cloudy/moist regions in the Tropics on the radiation energy balance. Although their result regarding so-called "infrared adaptive iris" hypothesis turned out to be very controversial and has been refuted (e.g., Lin et al. 2002; Hartmann and Mechelsen 2002; Fu et al.

---

*Corresponding author address:* Prof. Byung-Ju Sohn, School of Earth and Environmental Sciences, Seoul National University, NS80, Seoul 151-747, Korea.  
E-mail: sohn@snu.ac.kr

2002; Chambers et al. 2002), water vapor redistribution associated with the convection change over the Tropics proved to be important to the understanding of the role of water vapor in the radiation energy balance, in particular over the Tropics.

Since the tropical subsidence region is directly linked to the tropical convection area through the large-scale mass overturning as shown in the relationship between divergent wind and UTH within the Walker circulation cell (Newell et al. 1996a,b; Stone et al. 2000), any convection changes over the lower latitudes will cause changes in subsidence intensity and/or the size of subsidence areas. Thus, it is of interest to examine (i) how tropical convection influences horizontal moisture variations through the large-scale circulation and (ii) how changes in convection areas have an impact on the water vapor greenhouse effect, in particular, due to changes of water vapor in the upper troposphere.

In this paper, we try to understand the evolution of moist and dry areas associated with convection changes in the Tropics using the *European Geostationary Meteorological Satellite (Meteosat-5)* measurements over the Indian Ocean. A novelty is the attempt to interpret its consequences on the longwave radiation energy balance. In doing so the Indian Ocean, as a domain of interest, is divided into three areas: the moist cloudy area, the moist clear area, and the dry area. Figure 1 shows locations and spatial scales of the three moisture areas. Our study invokes the notion that the domain-dependent water vapor redistribution caused by convective activities in the Tropics should be an important mechanism modulating the radiation balance. We will examine the impact of areal changes of the dry upper troposphere on the water vapor greenhouse effect by relating upper-tropospheric humidity (UTH) changes to convection changes over the Tropics. In this paper, we first derive a relationship between the domain-averaged UTH and tropical convection. The results will then be used to examine the radiation energy balance arising from the redistribution of upper-tropospheric humidity associated with tropical convection.

## 2. Data and analysis

In this study, we use UTH retrievals from the water vapor channel (5.7–7.1  $\mu\text{m}$ ) measurements, in addition to cloud observations from the *Meteosat-5* located at 63°E over the Indian Ocean. The definition of UTH used in this study is an effective relative humidity with respect to water in the upper-tropospheric layer between about 200 and 500 hPa, with a maximum contribution from  $\sim 350$  hPa level.

Over the Indian Ocean, climatology shows that the intertropical convergence zone (ITCZ) is located in the equatorial area during Northern Hemisphere winter, implying that UTHs in both the north and south Indian Ocean in that season are largely controlled by tropical convection through the Hadley-type circulation (see Fig.

2 for the location of the ITCZ). By contrast UTH variations during the summer are more complex to interpret over the Indian Ocean analysis domain because the Hadley cell may not be located within the analysis domain so that convective activity over the Tropics may not be directly related to UTH variations over the Indian Ocean analysis domain. Because of these considerations and data availability we use two winter months (January and February 1999) of *Meteosat-5* data to determine the UTH variations in the Indian Ocean domain associated with tropical convection.

The *Meteosat-5* satellite data were extracted as rectified images from the Meteorological Archive and Retrieve Facility (MARF) at the European Organisation for the Exploitation of Meteorological Satellite (EU-METSAT). The radiometric measurements from the infrared window (IR: 10.5–12.5  $\mu\text{m}$ ) and water vapor (WV: 5.7–7.1  $\mu\text{m}$ ) channels were used; the spatial resolution of the measurements is about 5 km  $\times$  5 km at the subsatellite point. UTHs are estimated from WV brightness temperature (TB) measurements by applying the logarithmic relationship proposed by Soden and Bretherton (1996):

$$\ln(\text{UTH}/p_0) = a + b\text{TB}, \quad (1)$$

where  $p_0$  is a reference pressure. Regression coefficients  $a$  and  $b$  in Eq. (1) were established by simulating brightness temperatures for the *Meteosat-5* WV channel using atmospheric profiles in the TIROS Operational Vertical Sounder (TOVS) Initial Guess Retrieval (TIGR) database (Scott et al. 1991) as inputs to an infrared radiative transfer model, as in Sohn et al. (2000).

It is important to note that the *Meteosat-5* operational WV calibration has been adjusted to account for a high bias of about 10%–15%, corresponding to a 2–3-K warm bias in brightness temperature. Pixel-based UTH values are derived except for areas where IR brightness temperatures are lower than 275 K. This criterion generally ensures that cloud-contaminated scenes are removed because the maximum weighting function of the WV channel is located in the upper troposphere between 200 and 500 hPa with a broad peak around 350 hPa. The threshold eliminates clouds occurring above  $\sim 700$  hPa; failure to do so would yield an upper troposphere that is too moist. An IR temperature of less than 260 K is taken as an indication of high-level clouds. Three to four rectified images per day, around 0000, 0400, 1200, and 1600 UTC, are used for 2 months (January and February) thus providing adequate sampling.

Detrainment of hydrometeors from high clouds is the main source of moisture in the upper troposphere. The close resemblance between the high cloud and UTH fields is clearly depicted in their means over the two-month period (Fig. 2). The similarity also suggests that the increased UTH by convection expands the horizontal extent of the moist area, and thus contracts the dry area. In order to examine the moist and dry area changes associated with convection, we divide the Indian Ocean

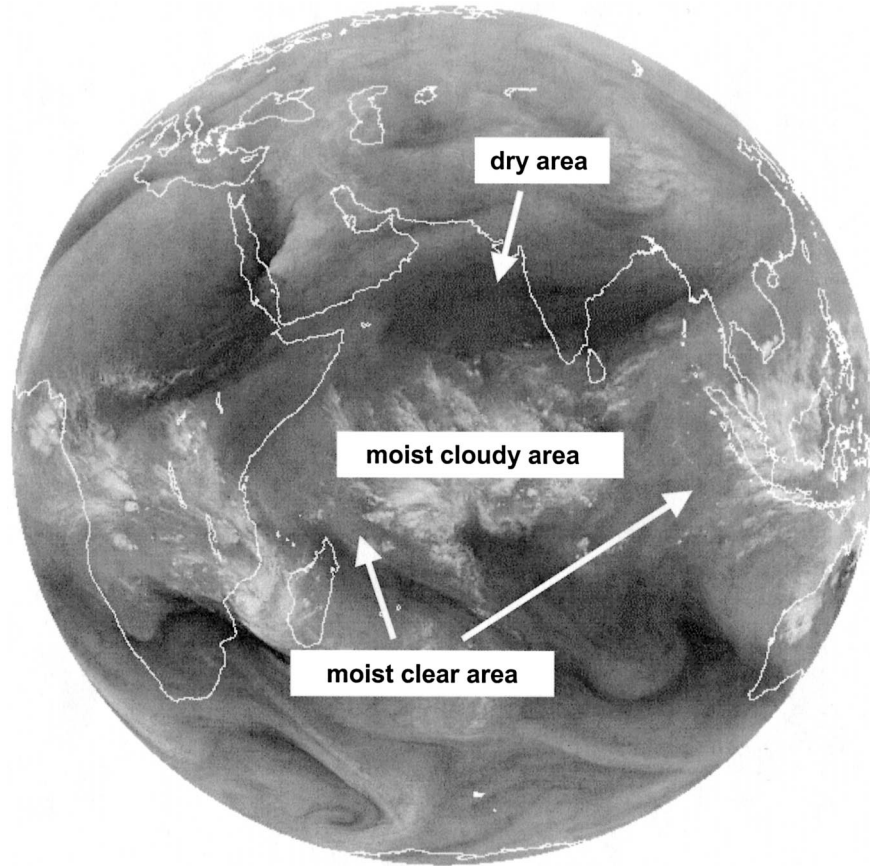


FIG. 1. *Meteosat-5* water vapor image from 15 January 1999. Dark areas for high brightness temperatures indicate cloud-free regions. High-level clouds appear in white. The inserts sketch the three areas referred in this paper: (i) moist cloudy area, i.e., areas of high-level cloud; (ii) moist-clear areas, i.e., areas of higher relative humidity that are moistened by dissolving clouds; and (iii) dry areas, i.e., areas not affected by clouds.

analysis domain into three different moisture regimes: a moist high cloud region ( $A_h$ ), a moist high cloud-free region ( $A_{mf}$ ), and a dry region ( $A_d$ ), as used in LCH for a 3.5 box model. The total area ( $A_t$ ) is then equal to ( $A_h + A_{mf} + A_d$ ). In what follows, we will interchangeably refer to the “high cloud area” of the Tropics as the “convective area” or “moist cloudy area” while referring to the “dry area” as the “subtropical dry region,” and referring to the “moist high cloud-free region” as “moist clear area.”

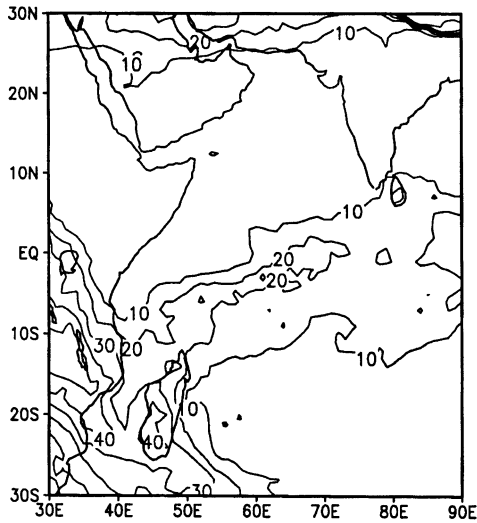
The humidities in the three areas differ from each other and, as stated above, potentially vary with the tropical convection and thus high-level cloud amount. Therefore UTH values need to be determined for the three areas. The moist clear area is defined by the high-cloud free pixels in a given  $1^\circ \times 1^\circ$  grid box (corresponding to about 480 pixels at the subsatellite point) where high cloud is present. The remaining boxes, having no high-cloud pixels, are taken to represent the dry area.

Since UTH retrievals from WV channel measurements are not possible from infrared radiation mea-

surements in the presence of high clouds, UTHs over the moist cloudy areas are replaced by the mean UTH value deduced from Special Sensor Microwave/Temperature-2 (SSM/T-2) aboard the Defense Meteorological Satellite Program (DMSP). Water vapor profiling and UTH retrievals from SSM/T-2 measurements are found in Engelen and Stephens (1999) and Sohn et al. (2003). The invariant UTH over the high cloud area may not be justified since the humidity within the cloud tends to be higher as the cloud size increases (Roca and Ramanathan 2000). However, because we examine humidity variations in terms of averages over three humidity regions, nearly invariant UTHs over the entire high cloud area may be acceptable, therefore, 56.7% of UTH obtained from SSM/T-2 measurements for January 1999 over the high cloud area is used for the UTH of the moist cloudy area.

The retrieval of UTH over the areas whose brightness temperatures are between 260 K and 275 K is mostly cloud contaminated; therefore the UTH over those areas is replaced by an average obtained from clear pixels within a given box. If no pixel greater than 275-K

### Meteosat 5 High Cloudiness ( Jan, Feb 1999 )



### Meteosat 5 UTH ( Jan, Feb 1999 )

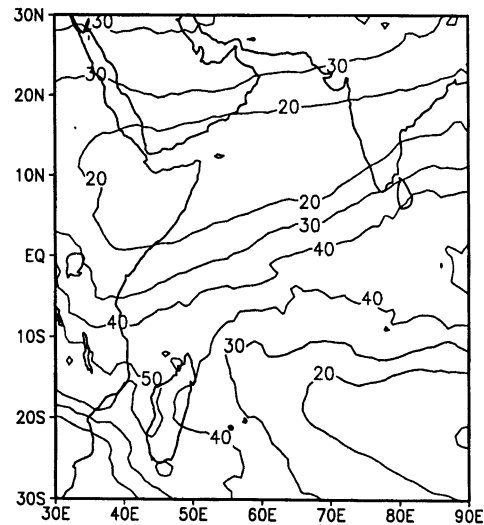


FIG. 2. Geographical distributions of (left) high-cloud amount and (right) upper-tropospheric humidity, averaged over the Jan–Feb 1999 period. Units are given in percent and both contour intervals are 10%.

brightness temperature is found with a given  $1^\circ \times 1^\circ$  grid box, then UTH in the closest surrounding boxes is used to assign the UTH for those areas.

Figure 3 shows a time series of the fractional area coverage for moist cloudy and moist clear areas from *Meteosat-5* images considered in this study. The third class “dry area” is just the difference between unity and the sum of moist cloudy and moist clear area fraction. In general, the figure shows that the moist clear area is proportional to the moist cloudy area. The average ratio between these two areas during this period was about 2 by this approach, although a factor of 2 relationship is not clear around the 35th image.

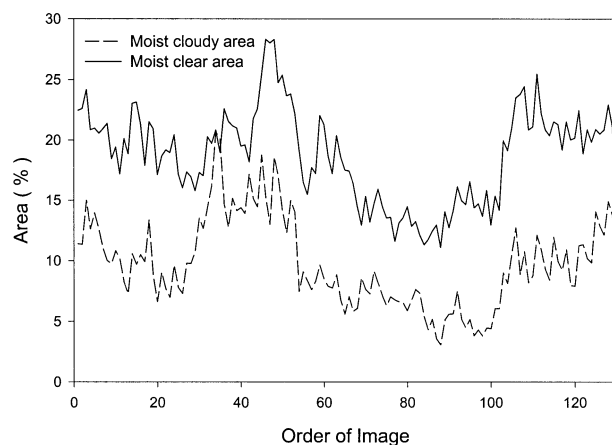


FIG. 3. The fractional area of the moist cloudy and moist clear regions. Number on the ordinate indicates the order of the 129 sequential images used in this study.

### 3. Relationship between UTH and tropical convection

An important question is how the actual values of humidity in the dry and moist clear areas vary with tropical convection changes, if they do so at all. We examined this by comparing the relationship between the high-cloud amount and UTH for dry and moist clear areas and for the total (see Fig. 4). In Fig. 4, the high-cloud amount is the percentage ratio of high-cloud area to the total analysis area and the corresponding UTH is a respective area mean. Since the ratio of moist clear area to high-cloud area is about 2 and the total area is fixed, an increase in high cloud implies an increase of the moist clear area by a factor of 2 times the increase of the moist cloudy area, and a corresponding decrease in the dry area.

In general, there is a decreasing trend of UTH for moist-clear and dry areas with respect to increases in high-cloud area. However, the slope of  $-0.17$  for this trend in the moist clear area (Fig. 4a) is relatively weak compared to  $-0.33$  for the dry area. Mean UTHs for moist clear and dry areas are around 47% and 23%, respectively. Here we should remember that the dry area is geographically separated from the convective area and represents the area of large-scale subsidence in the subtropics. The observed linear relationship between high-cloud area over the Tropics and UTH over the subtropics strongly suggests that the subtropical regions become drier when the tropical moist area expands, although the areal coverage of the dry area decreases. Considering the fact that the OLR flux changes for a given UTH change are most sensitive when the upper troposphere

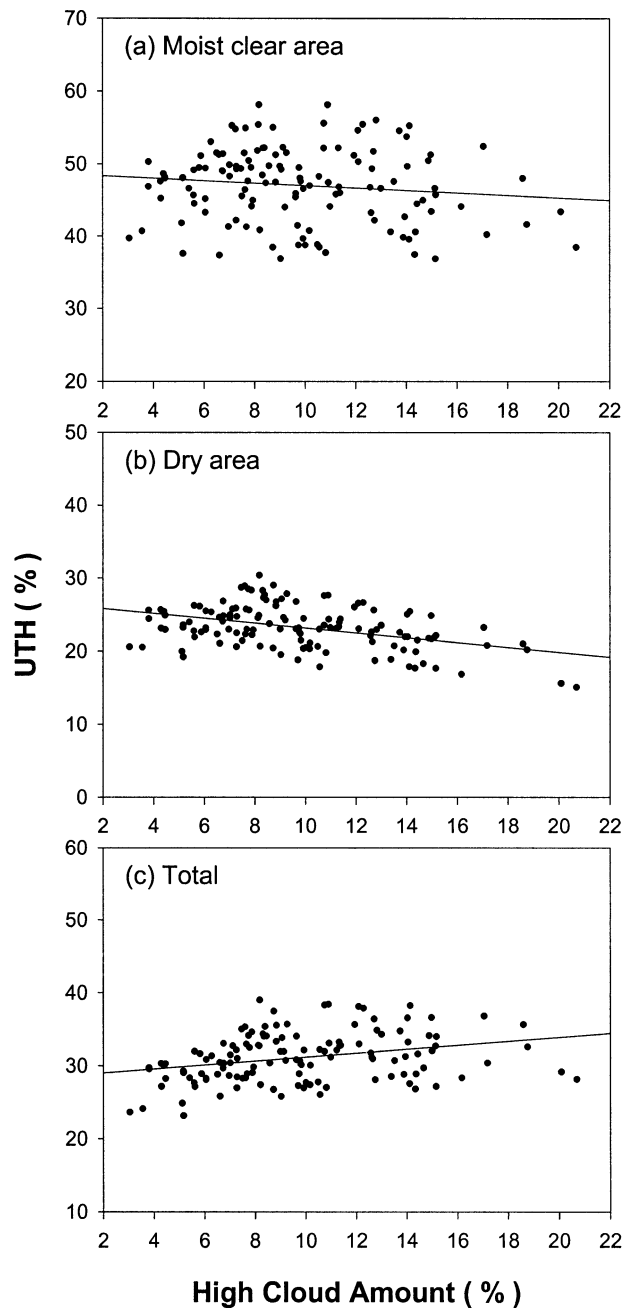


FIG. 4. Scatterplots of high-cloud area vs mean UTH for (a) moist clear area, (b) dry area, and (c) total. Each data point corresponds to one *Meteosat-5* image.

is dry, it is the dry subtropical area that gives rise to the most significant influences on OLR fluctuations. Thus, in the subtropics there seem to be two competing mechanisms with regard to the OLR changes. The shrinking of the dry area leads to a decrease in the OLR and thus a corresponding increase in the greenhouse effect, whereas the drying itself enhances transmissivity and weakens the greenhouse effect.

Figure 4c exhibits the net result of the area and corresponding UTH changes obtained by applying the proper weighting for area coverage. Overall, we observe an UTH increase over the total area with an increased high-cloud area. This is mainly due to the increased coverage of moist area (moist cloudy plus moist clear area), indicating that the overall effect of convection over the Tropics is to humidify the upper troposphere in the domain-average sense. Such a positive relationship has been noted in previous studies (e.g., Soden and Fu 1995; Chen et al. 1999; Sassi et al. 2001).

The relationship of dry regions to the tropical convection is summarized in Fig. 5. The Tropics is thought of as a region of net ascent, while the subtropics is a region of descent, and these two regions are linked to each other by a Hadley-type circulation. As seen in the diagram, we postulate that the fractional area of the dry region changes in response to convection changes in the Tropics. Enhanced convection over the Tropics will be followed by an expansion of the moist area, with consequent evaporation of hydrometeors from cumulus towers, while the optically thin dry area contracts in response to the expansion of the moist area. Of special importance is the drying of the upper troposphere in the descending dry region. Based on the mean descending motion and the lack of cumulus convection in the dry region, vertical transport associated with increased descending motion appears to be the main agent supplying dry air to lower layers. In accordance with this strengthened mean descent, it is presumed that the underlying inversion becomes stronger and the moisture in the shallower boundary layer is transported more easily to convective regions where latent heat is released. Opposite behavior can be expected from other conditions; that is, a reduced convection area in the Tropics leads to moister conditions in the subtropical free atmosphere.

#### 4. WV greenhouse effect influenced by convection changes over the Tropics

The final purpose of this study is to assess the overall effect on the longwave trapping when moist/dry area changes occur as observed over the Indian Ocean. We calculate the OLR changes on the basis of a parameterization of individual fractional area as a function of high-cloud area ( $A_h$ ). This is possible because the fractional areas of moist clear ( $A_{mf}$ ) and dry regions ( $A_d$ ) can be expressed in terms of the fractional area of tropical deep convection. The moist clear area fraction is set to be  $2A_h$  and thus the remaining dry area is  $(1 - 3A_h)$ . Respective UTHs are specified on the mean basis of the observations. To examine the impact of the varying UTHs in the moist clear and dry regions, we adopt two scenarios: (i) UTHs for three areas are fixed using respective mean values and (ii) UTHs for moist clear and dry areas vary as a function of high-cloud area, as determined from the *Meteosat-5* observations in Figs.

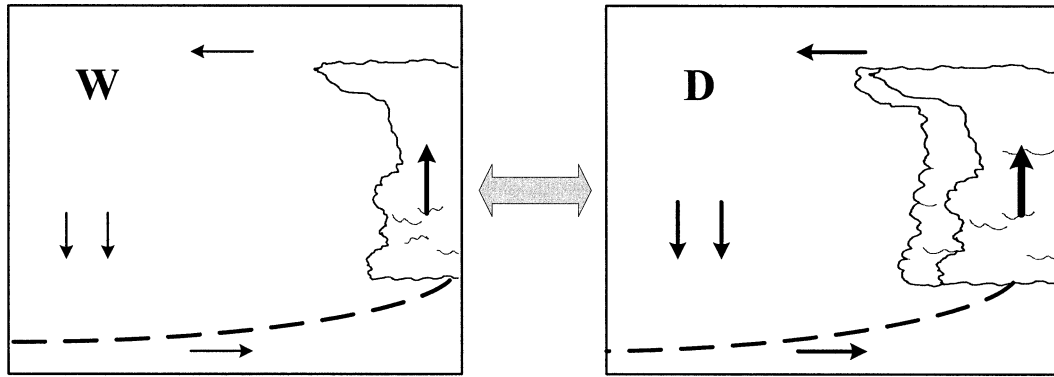


FIG. 5. Schematic diagram showing decreased (or increased) cloud area in the Tropics and associated moistening (or drying) effect in the subtropics. Arrows indicate the direction of the Hadley circulation and the dashed line represents the top of the boundary layer; **W** and **D** represent relatively wetter and drier subtropical upper troposphere, respectively. The thicker arrows in the right panel indicate strengthened circulation intensity.

4a,b. A schematic diagram for this three-area model as a function of high-cloud area is given in Fig. 6.

For the OLR calculation we construct the mean atmospheric conditions using the National Centers for Environmental Prediction–National Center for Atmospheric Research (NCEP–NCAR) reanalysis data for the period under study. Temperature and moisture profiles are averaged over the latitude belt 10°N–10°S for the tropical convection area and in 20°–30° latitude belts in both hemispheres for the subtropical dry area. Mean atmospheric profiles for the moist clear area are then estimated by taking the average of the two mean profiles. The water vapor greenhouse effect is then estimated from radiative transfer calculations for a fixed relative humidity equal to the observed UTH in an atmospheric layer between 4 and 12 km, while the lower troposphere is kept at the mean atmospheric conditions from the NCEP data. The radiative transfer calculations are performed with a narrowband model that considers all relevant gaseous atmospheric absorbers (Smith and Shi 1992). The water vapor greenhouse effect is computed in the usual way as the difference between OLR at the

top of the atmosphere and the outgoing longwave flux at the surface.

The calculated greenhouse effects due to the water vapor burden for the three regions are given in Fig. 7 as a function of UTH. Comparing the greenhouse effect for the dry region ( $G_d$ ) with those for the moist clear ( $G_{mf}$ ) and moist cloudy regions ( $G_h$ ), it is seen that the dry region is most sensitive to small changes in UTH. Significant nonlinear sensitivity is evident for the dry region whereas nearly linear trends exist for both the moist clear and moist high-cloud regions. Therefore, it is the optically thin dry region that exerts more influence on the water vapor greenhouse effect, rather than the optically thick moist regions. However, the absolute magnitude of the greenhouse effect grows progressively larger from the dry region to the moist cloudy region.

Figure 8 summarizes the results of the radiative transfer calculation for the three areas and their sum as a function of high-cloud amount (i.e., as a function of tropical deep convection). The area-mean greenhouse effect in the total domain ( $G_t$ ) is obtained from the area-weighted means:

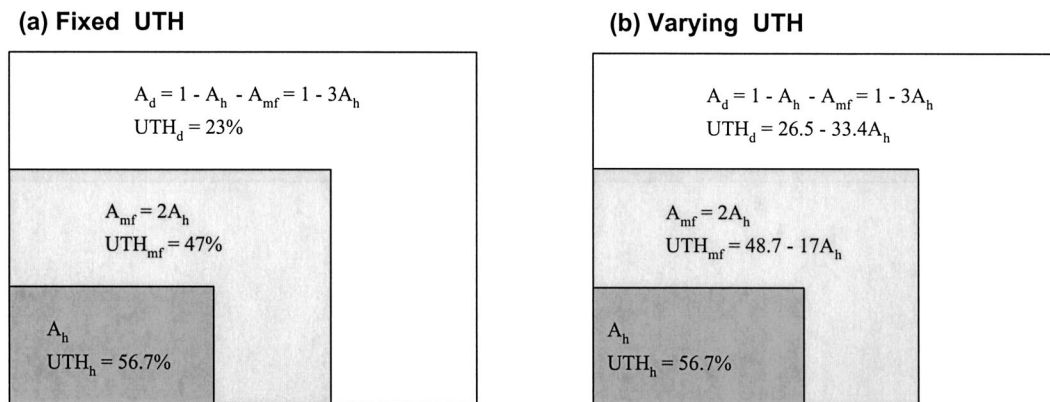


FIG. 6. Schematic diagrams showing (a) fixed UTH and (b) varying UTH model used for radiative transfer calculations;  $A_h$ ,  $A_{mf}$ , and  $A_d$  represent areas for moist cloudy, moist clear, and dry regions, respectively. See text for details.

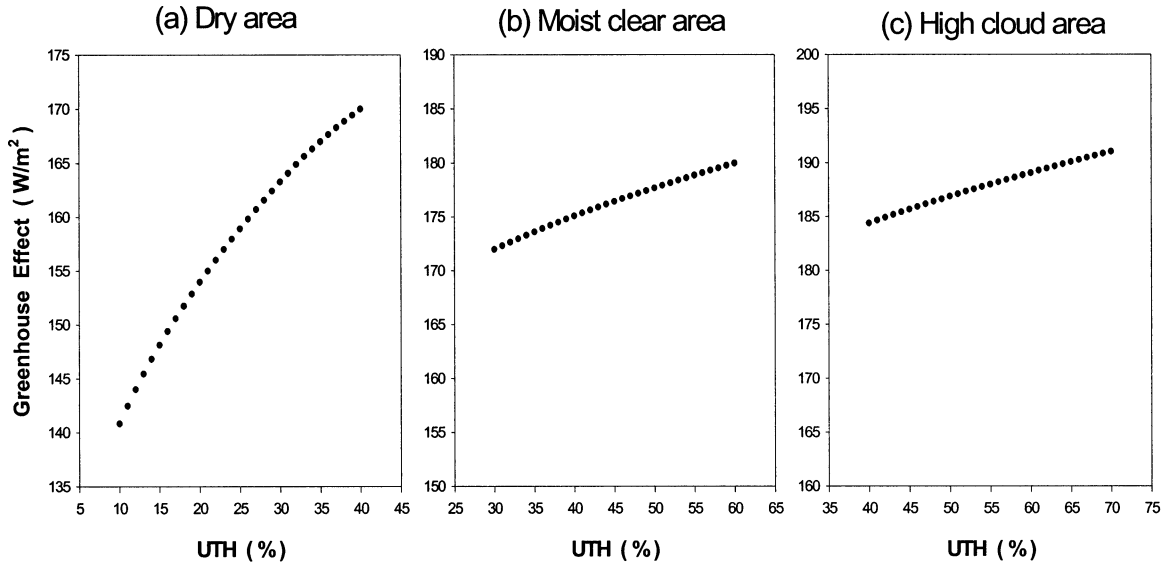


FIG. 7. Greenhouse effect as a function of UTH in the upper layer between 4 and 12 km for (a) dry, (b) moist clear, and (c) moist cloudy region.

$$G_t = A_h G_h + A_{mf} G_{mf} + A_d G_d, \quad (2)$$

where  $A_h$ ,  $A_{mf}$ , and  $A_d$ , are the fractional coverages of the moist cloudy, the moist clear, and the dry areas, respectively. Here  $G_h$ ,  $G_{mf}$ , and  $G_d$  represent the corresponding greenhouse effects over those three areas. Since  $A_{mf}$  and  $A_d$  can be expressed using  $A_h$ , the total

greenhouse effect can also be expressed as a function of  $A_h$ :

$$G_t = A_h G_h + 2A_h G_{mf} + (1 - 3A_h) G_d. \quad (3)$$

In Fig. 8, it is shown that the largest contribution to the total greenhouse effect is from the subtropical dry area because of its large fractional area. Furthermore, the largest variation of the greenhouse effect is also found in the subtropical dry area. This is due to the fact that the dry area is linked to the convective area by a factor of 3, resulting in rapid areal change relative to changes in the moist areas. Other important factors to consider for the varying greenhouse effect are the magnitude of the change (slope) of UTH with respect to high-cloud amount and the sensitivity of the greenhouse effect to UTH variation. It is the subtropical dry area that shows the largest slope, highest sensitivity, and most rapidly varying area with respect to changes in high-cloud amount, all of which give rise to the largest contribution to the total. However, the net result is an enhanced greenhouse effect as convection increases because of the increased moist area in the Tropics.

Although the total greenhouse effect is dominated by changes in high-cloud area, the varying dryness of clear areas (dry area plus moist clear area) tends to mitigate the impact of area changes as shown in Table 1. When mean values of high-cloud area and UTH are used, the total greenhouse effect is  $163.9 W m^{-2}$ . With a 1% increase of high-cloud area, the variations of total water vapor greenhouse effect are about 0.71 and  $0.46 W m^{-2}$  for the fixed and varying UTH, respectively. Thus  $0.25 W m^{-2}$  of the difference represents the decreased greenhouse effect due to the now drier atmospheric conditions in the smaller dry area. On the other hand, an increased warming with a similar magnitude may be

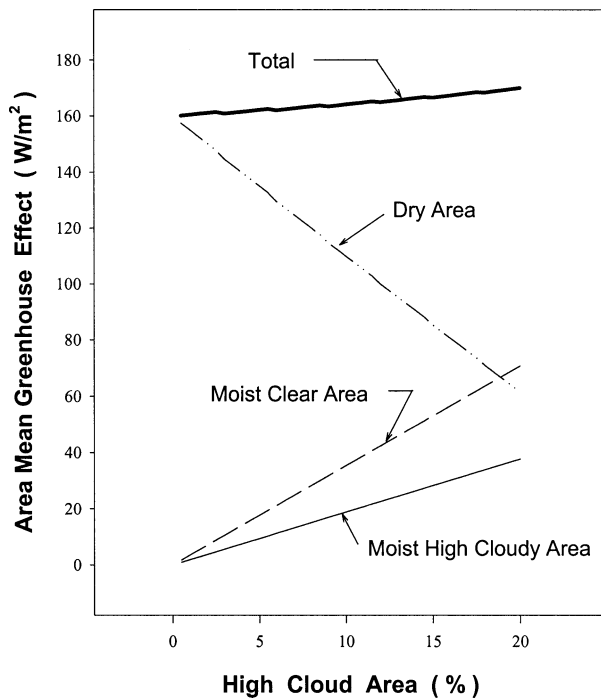


FIG. 8. Area mean greenhouse effect (dashed) contributed by moist cloudy (solid), moist clear (broken), and dry area (dashed and dotted) as a function of high-cloud area.

TABLE 1. The total greenhouse effect ( $G_t$ ) averaged over the Indian Ocean domain at the mean condition, and the variation of greenhouse effect with respect to the high-cloud amount change ( $\text{W m}^{-2}$  per percent) for the two UTH prescriptions.

	$G_t$ ( $\text{W m}^{-2}$ ) at $A_h = 9.8\%$	$\frac{dG_t}{dA_h}$ ( $\text{W m}^{-2}/\%$ )
Fixed UTH	163.9	0.71
Varying UTH	163.9	0.46

found when the cloud area is shrunken due to the now wetter conditions in the much expanded dry region. This result suggests that dryness changes in the subtropical high pressure region counteract the cooling (warming) due to the reduction (expansion) of the moist area in the Tropics.

Before drawing any firm quantitative conclusions from above analysis, further studies are warranted because the moist-clear area as well as dry area and their respective UTHs are sensitive to the chosen grid size. The sensitivity analysis of greenhouse effect to the chosen spatial resolution is provided in the appendix.

## 5. Discussion on water vapor area (iris) feedback

Recently, LCH reported observational analyses showing that high-cloud areas over the tropical western Pacific are negatively correlated with the average sea surface temperature (SST) underneath the high clouds. Although their so-called iris hypothesis was questioned and objected by other studies (e.g., Lin et al. 2002; Hartmann and Michelsen 2002; Fu et al. 2002; Chambers et al. 2002), it is interesting to examine whether the water vapor area changes associated with convection changes are incorporated in their model and thus whether their water vapor feedback sensitivity reflects features noted in this study. Our study also addresses questions of the sensitivity of the contemporary climate to relative changes in the fractional areas of cloudy/moist regions in the Tropics.

An important result we could infer from Fig. 8 is that the overall area feedback is weak. LCH argued that a 1-K increase in SST of the tropical cloudy area induces an approximate 22% decrease in high-cloud amount. Adopting this value, we can examine how strong the water vapor feedback of the contemporary climate would be for a given change in high-cloud area. Following the notation of LCH, the response of the climate system ( $\Delta T$ ; here in the tropical system) to water vapor area feedback can be expressed as

$$\Delta T = G_0(\Delta Q + F\Delta T), \quad (4)$$

where  $\Delta Q$  and  $G_0$  are a radiative forcing and no-feedback gain, respectively, and  $G_0 F$  is the feedback factor. For the tropical atmosphere,  $G_0$  can be determined by considering the flux ( $Q_E$ ) change associated with equilibrium temperature ( $T_E$ ) change; that is,  $\Delta Q_E/\Delta T_E = 4\sigma T_E^3$ , where  $\sigma$  is the Stephan–Boltzmann constant. For

the LCH equilibrium temperature for a tropical clear-moist atmosphere,  $T_E = T_s - 37$ , where  $T_s$  is the SST. Considering a tropical SST of 300 K,  $G_0$  is  $(4.13 \text{ W m}^{-2})^{-1}$ .

When fixed UTHs are assumed for the three regions, modeling results indicate that a 22% decrease of high-cloud amount in response to a 1-K SST change, as in LCH, results in a longwave radiation reduction of  $1.3 \text{ W m}^{-2}$  that corresponds to a negative water vapor feedback of  $-0.31$ . This negative feedback becomes less significant with  $-0.18$  when UTHs values are allowed to vary according to observations. LCH did not account for such UTH variations, particularly within the dry region. LCH reported a negative feedback factor of  $-1.1$  from the combined cloud and water vapor influence and a feedback factor of  $-0.45$  due to clouds alone. Thus a feedback factor due to water vapor coupled with clouds would be  $-0.65$ . Compared to the water vapor feedback factor  $-0.65$ , our result indicates a much smaller negative feedback although the analysis domain and period are different from those employed in LCH.

## 6. Summary and conclusions

Examining the impact of horizontal variations of upper-tropospheric humidity on the water vapor greenhouse effect over the Indian Ocean, the analysis domain was divided into three different moisture regimes: a moist cloudy region, a moist clear region, and a dry region using the *European Geostationary Meteorological Satellite (Meteosat-5)* measurements. The variations in UTHs for the moist clear region and dry region are compared with convection changes over the Tropics.

It is indicated that fluctuations in moist clear area are similar to those of the high-cloud area, suggesting that the moist clear area tends to be proportional to the size of convective region. In this study, employing a  $1^\circ \times 1^\circ$  gridbox resolution, the ratio between these two areas during the January–February 1999 analysis period is about 2. It is obvious that the dry region should be decreased accordingly because the total area is fixed. Furthermore, it was found that both dry and moist clear areas undergo humidity changes in response to changes in the convective area; there is a decreasing trend of UTH for both moist clear and dry areas with respect to increases in high-cloud area. The negative relationship between high-cloud area over the Tropics and UTH over the subtropics suggests that the subtropical regions become drier when the tropical moist area expands, although the areal coverage of the dry area decreases. Such dryness changes over the subtropics as well as over the moist clear area appear to counteract the increase in water vapor greenhouse effect caused by the expansion of moist convective areas.

In order to examine the water vapor greenhouse effect associated with area and humidity changes in the three regions, we calculated OLR changes on the basis of a parameterization of fractional area as a function of high-



cloud area. Results indicate that variations of the total greenhouse effect are dominated by changes in high-cloud area, but the varying dryness within clear areas (dry area plus moist clear area) tends to mitigate the impact of area changes. Assuming a 1% increase of high-cloud area, the total water vapor greenhouse effect is increased by about  $0.71 \text{ W m}^{-2}$  for the fixed UTHs and by  $0.46 \text{ W m}^{-2}$  for the varying UTHs, resulting in a lower greenhouse effect decreased by  $0.25 \text{ W m}^{-2}$  due to the drier atmospheric conditions over dry and moist clear areas. In conclusion, the dryness changes in the subtropics mitigate the greenhouse cooling (warming) due to the reduction (expansion) of the moist cloudy area in the Tropics.

Including this result in the area feedback calculations for the contemporary climate provides quite a benign feedback of only  $-0.18$  over the Indian Ocean, assuming the high cloud is reduced by 22%. Although the feedback factor obtained in this study cannot be directly compared with the LCH value because of the different analysis domain and period, it is likely that their value was overestimated due to the neglect of humidity variations in the dry region in response to convection changes over the Tropics. Although this study is based on a rather small dataset, it supports the notion of a negative water vapor area feedback as put forward by LCH. However, it also demonstrates that the magnitude of this water vapor area feedback is likely to be quite benign.

*Acknowledgments.* The authors wish to thank Dr. Eugene McCaul for carefully reading the manuscript and Mr. Eui-Seok Chung for data processing and Drs. Marianne König and Hans Jochim Lutz for helpful discussions on various scientific problems. The first author has been supported by the Climate Environment System Research Center, sponsored by the SRC Program of the Korea Science and Engineering Foundation, and by the BK21 Project of the Korean government. This research was performed while the first author was at EUMETSAT as a visiting scientist.

## APPENDIX

### Sensitivity to the Chosen Grid Size

It is apparent that the moist clear area as well as dry area and their respective UTHs are sensitive to the horizontal resolution of data. For example, if a pixel-size grid with a  $\sim 5 \text{ km}$  resolution is used, the moist clear area will nearly vanish since each pixel will be mostly classified as either moist cloudy area or clear-sky area. It is a matter of what criteria for UTH would be applied to determine the moist clear area since dry area and moist clear area complement each other.

Udelhofen and Hartmann (1995) provide some evidences of what horizontal scale might be appropriate to separate the moist clear area from the dry area. Using

TABLE A1. Sensitivity of  $dG_i/dA_n$  to the area and UTH changes in the dry region associated with grid size changes. The ratios were arbitrarily altered.

Ratio of UTH increase	Ratio of dry area increase				
	-10%	-5%	0%	5%	10%
-10%	0.49	0.50			
-5%	0.46	0.48	0.49		
0%		0.44	0.46	0.48	
5%			0.43	0.45	0.46
10%				0.42	0.43

the Geostationary Operational Environmental Satellite (GOES-7)  $6.7\text{-}\mu\text{m}$  channel measurements they examined the horizontal variations of UTH from the cloud edge and obtained the best fit describing the horizontal humidity variation over the Tropics ( $15^\circ\text{N}$ – $15^\circ\text{S}$ ,  $142.5^\circ$ – $52.5^\circ\text{W}$ ) as a function of distance ( $r$ ) from the cloud edge; that is,  $\text{UTH}(r) = 56.8 \exp(-0.091 r^{1/2}) + 9.2$ . Thus, on average, UTHs at the cloud edge ( $r = 0$ ),  $r = 50 \text{ km}$ ,  $r = 100 \text{ km}$ , and  $r = 200 \text{ km}$  are to be 66.1%, 39%, 32%, and 24%, respectively, showing that UTHs decrease rapidly within 50 km from the cloud edge. These findings suggest that most of the moist region in the vicinity of high-cloud area may be captured when  $1^\circ \times 1^\circ$  grid boxes are used.

In order to assess the credibility of the changes in water vapor greenhouse effect associated with convection changes in the Tropics, we have carried out sensitivity tests addressing how the results are affected by the chosen grid size. We first investigated how dry areas are changed with varying grid sizes from the current  $1^\circ$  resolution to finer  $0.5^\circ$  and coarser  $1.5^\circ$  grid resolution. Analysis of one randomly chosen *Meteosat-5* image shows that the relative increase of the dry area is 11% from 72% to 80% when the resolution is changed from  $1^\circ$  to  $0.5^\circ$  while the corresponding UTH is increased by about 6% from 18% to 19%. On the other hand, the dry area and associated UTH are decreased by 9% and 5%, respectively, when the grid resolution is changed from  $1^\circ$  to  $1.5^\circ$ . Using this result as a reference, we allow the dry area obtained from the  $1^\circ \times 1^\circ$  grid box approach to change arbitrarily by  $r\%$ . As a result new areas for the dry clear and moist clear region will emerge because the cloud area is invariant with the chosen grid box:

$$A'_d = A_d(1 + r/100) \quad (\text{A1})$$

$$A'_{mf} = 1 - A'_d - A_h, \quad (\text{A2})$$

where primes denote altered value. Then we assume that the mean UTH over the dry area is accordingly increased by  $s\%$  in response to the dry area increased by  $r\%$ . Given the mean UTH for the total area as a function of high cloud (see Fig. 4c), the mean UTH for the moist clear region can be determined.

Radiative transfer calculations, as in section 4, were repeated with new values of dry and moist clear areas and their corresponding UTHs. Table A1 summarizes

changes in  $dG_i/dA_h$ , in response to variations in the size of dry area and UTH caused by chosen grid size. Only diagonal parts are presented in Table A1 since the area change is positively correlated with the UTH change. It is noted that for the given dry area and UTH changes, the resultant  $dG_i/dA_h$  varies only between 0.42 and 0.50 and therefore is not significantly different from  $dG_i/dA_h = 0.46$  as determined for the  $1^\circ \times 1^\circ$  grid resolution. Thus, our interpretation of water vapor-induced OLR and greenhouse changes associated with high cloud variations over the Tropics remains unchanged.

## REFERENCES

- Chambers, L. H., B. Lin, and D. F. Young, 2002: Examination of new CERES data for evidence of tropical iris feedback. *J. Climate*, **15**, 3719–3726.
- Chen, M., R. B. Rood, and W. G. Read, 1999: Seasonal variations of upper tropospheric water vapor and high clouds observed from satellites. *J. Geophys. Res.*, **104**, 6193–6197.
- Engelen, R., and G. L. Stephens, 1999: Characterization of water-vapour retrievals from TOVS/HIRS and SSM/T-2 measurements. *Quart. J. Roy. Meteor. Soc.*, **125**, 331–351.
- Fu, Q., M. Baker, and D. L. Hartmann, 2002: Tropical cirrus and water vapor: An effective Earth infrared iris feedback. *Atmos. Chem. Phys.*, **2**, 31–37.
- Hartmann, D. L., and M. L. Michelsen, 2002: No evidence for iris. *Bull. Amer. Meteor. Soc.*, **83**, 249–254.
- Houghton, J. T., Y. Ding, D. J. Griggs, M. Noguer, P. J. van der Linden, X. Dai, K. MasKell, and C. A. Johnson, Eds., 2001: *Climate Change 2001: The Scientific Basis*. Cambridge University Press, 867 pp.
- Inamdar, A. K., and V. Ramanathan, 1998: Tropical and global scale interactions among water vapor, atmosphere greenhouse effect, and surface temperature. *J. Geophys. Res.*, **103**, 32 177–32 194.
- Larson, K., D. L. Hartmann, and S. A. Klein, 1999: On the role of clouds, water vapor, circulation and boundary layer structure on the sensitivity of the tropical climate. *J. Climate*, **12**, 2359–2374.
- Lin, B., B. A. Wielicki, L. H. Chambers, Y. Hu, and K.-M. Xu, 2002: The iris hypothesis: A negative or positive cloud feedback? *J. Climate*, **15**, 3–7.
- Lindzen, R. S., M.-D. Chou, and A. Y. Hou, 2001: Does the Earth have an adaptive infrared iris? *Bull. Amer. Meteor. Soc.*, **82**, 417–432.
- Newell, R. E., Y. Zhu, E. V. Browell, S. Ismail, W. G. Read, J. W. Waters, K. K. Kelly, and S. C. Liu, 1996a: Upper tropospheric water vapor and cirrus: Comparison of DC-8 observations, preliminary UARS microwave limb sounder measurements and meteorological analyses. *J. Geophys. Res.*, **101**, 1931–1941.
- , —, —, W. G. Read, and J. W. Waters, 1996b: Walker circulation and tropical upper tropospheric water vapor. *J. Geophys. Res.*, **101**, 1961–1974.
- Raval, A., and V. Ramanathan, 1989: Observational determination of the greenhouse effect. *Nature*, **342**, 758–761.
- Roca, R., and V. Ramanathan, 2000: Scale dependence of monsoonal convective systems over the Indian Ocean. *J. Climate*, **13**, 1286–1298.
- Sassi, F., M. Salby, and W. G. Read, 2001: Relationship between upper tropospheric humidity and deep convection. *J. Geophys. Res.*, **106**, 17 133–17 146.
- Schmetz, J., and Coauthors, 1995: Monthly mean large-scale analyses of upper-tropospheric humidity and wind field divergence derived from three geostationary satellites. *Bull. Amer. Meteor. Soc.*, **76**, 1578–1584.
- Scott, N., and Coauthors, 1991: Recent advances in the 3d thermodynamic analysis of the earth system through the “3I” algorithm: Extension to the second generation vertical sounders. *Tech. Proc. Sixth Int. TOVS Study Conf.*, Airlie, VA, IAMAS, 425–467.
- Sherwood, S. C., 1999: On moistening of the tropical troposphere by cirrus clouds. *J. Geophys. Res.*, **104**, 11 949–11 960.
- Smith, E. A., and L. Shi, 1992: Surface forcing of the infrared cooling profile over the Tibetan Plateau. Part I: Influences of relative longwave forcing at high latitude. *J. Atmos. Sci.*, **49**, 805–822.
- Soden, B. J., and R. Fu, 1995: A satellite analysis of deep convection, upper-tropospheric humidity, and the greenhouse effect. *J. Climate*, **8**, 2333–2351.
- , and F. P. Bretherton, 1996: Interpretation of TOVS water vapor radiances in terms of layer-average relative humidities: Method and climatology for the upper, middle, and lower troposphere. *J. Geophys. Res.*, **101**, 9333–9343.
- Sohn, B. J., J. Schmetz, S. Tjemkes, M. Koenig, A. Arriaga, and E. S. Chung, 2000: Intercalibration of Meteosat-7 water vapor channel with SSM/T2. *J. Geophys. Res.*, **105**, 15 673–15 680.
- , E. S. Chung, J. Schmetz, and E. A. Smith, 2003: Estimating upper tropospheric water vapor from SSM/T-2 measurements. *J. Appl. Meteor.*, **42**, 488–504.
- Stephens, G. L., 1990: On the relationship between water vapor over the oceans and sea surface temperature. *J. Climate*, **3**, 634–645.
- Stone, E. M., L. Pan, B. J. Sandor, W. G. Read, and J. W. Waters, 2000: Spatial distributions of upper tropospheric water vapor measurements from the UARS Microwave Limb Sounder. *J. Geophys. Res.*, **105**, 12 149–12 161.
- Udelhofen, P., and D. L. Hartmann, 1995: Influence of tropical convective cloud systems on the relative humidity in the upper troposphere. *J. Geophys. Res.*, **100**, 7423–7440.